Controlling Crystal Orientation of 2D Bismuth Triiodide (BiI_3) via Close-space Sublimation Processing for Use in Non-toxic, Low-temperature Thin Film Solar Cells

A Major Qualifying Project
Submitted to the Faculty and Staff of
WORCESTER POLYTECHNIC INSTITUTE
in partial fulfillment of the requirements for the
Degrees of Bachelor of Science in Chemical Engineering

By

James McRae

Professor Pratap Rao, Advisor

Abstract

BiI_3 has favorable photovoltaic properties with an ideal band gap of 1.8 eV and potential processing through evaporation. There has been much research done on solution-processing BiI_3 for photovoltaics. However, BiI_3 thin films can be fabricated using evaporation techniques as well. Our group has developed a close-space sublimation (CSS) technique for consistently fabricating BiI_3 films with control over the crystal orientation. When fabricated by solution processing, the crystals orientation is random. However, CSS provides control over vertical or horizontal orientation. When evaporating, moderating the source-substrate temperature difference results in the variance of crystal orientation, with a large temperature difference resulting in vertical crystals, and a small difference resulting in horizontal crystals.

No literature exists on evaporated BiI_3 in functioning solar cells. Our group has fabricated functioning solar cells using CSS-fabricated, vertically oriented BiI_3 as the absorber layer. We hypothesize that vertically oriented BiI_3 will enable easier charge transport due to fewer grain boundaries compared to other orientations, thus increasing efficiency.

Further experimentation will focus on source temperature, time, and annealing conditions. Samples will be characterized using SEM, Absorbance measurements, and quantum efficiency measurements. Full cells will undergo performance testing.

Acknowledgements

First and foremost, we would like to thank our advisor Professor Pratap Rao who's guidance and constructive criticism helped make this project possible. His knowledge regarding solar cells played a significant role in the thought-process as well as the final experiments of our research. Also, we would like to thank the graduate students in Higgins Laboratories' NanoEnergy Lab, particularly Binod Giri, Sunhao Liu, and Nick Pratt.

Additionally, we would like to thank the staff of the Physics Department, particularly Nancy Burnham and Professor Obayemi, who helped us perform SEM on our samples. Lastly, we would like to thank Agata Lajoie who greatly helped us navigate and attend the National Conference on Undergraduate Research (NCUR) where we will be able to present our research.

Table of Contents

List of Figures

Chapter 1: Introduction

Solar energy provides a viable alternative to fossil fuels, the current predominant source of energy. There are various types of solar cells in the market as well as being researched. Silicon-based cells, perovskite-based cells, CdTe cells, CIGS cells, and polymer-based cells are the most common types of solar cells, while other cells with the absorber materials BiI_3 and MBI have shown great promise. The reason for researching the different types of solar cells is to create a more competitive solar energy market and produce solar cells that have high power conversion efficiency, longer lifespan, are non-toxic, and are easily manufacturable.

The main focus of this research is on the use of BiI_3 as an absorber layer in solar cells. BiI_3 has a band gap of 1.8 eV, making it suitable as a standalone solar cell or as a tandem solar cell to be paired with commercial silicon cells, which have a band gap of 1.1 eV. BiI_3 is easily processable by many techniques such as solution processing (soluble in many solvents) and evaporation deposition (sublimes at low temperatures). Additionally, in evaporation deposition processes, the crystal orientation of BiI_3 can be controlled by adjusting the temperature difference between the source and substrate.

One of the most important characteristics of BiI_3 is that it has a two-dimensional layered crystal structure, meaning that the stacks of crystals are held together by weak molecular interactions (Brandt et al). When the crystals are oriented horizontally, the excited charges have to travel through many grain boundaries, potentially hindering the overall performance of the solar cell. However, if the crystals are oriented vertically, the excited charges would be able to travel through the vertical single crystals with greater ease, potentially improving performance.

This project will attempt to achieve the following three objectives, which the team believes will result in a better understanding and improved control over BiI_3, as an absorber material, but also an improved solar cell produced by methods feasible and commonly used in commercial manufacturing:

1. Develop procedures for controlling the orientation of BiI_3 crystals via close-spaced sublimation (CSS).
2. Identify which BiI_3 crystal orientation will allow for improved charge transport and increased efficiency.
3. Improving the overall cell performance through techniques such as annealing and modifying the hole transport layer.

Chapter 2: Motivation

The motivation chapter covers information regarding the importance of making technological advances in the renewable energy industry. The current technology and limitations of various types of solar cells are detailed, specifically silicon and lead-based solar cells. Lastly, the benefits, current technology, and limitations of BiI_3 are described.

2.1 Current Energy Demands

The following section provides information regarding the current energy usage, particularly in the United States, the challenges that exist when trying to switch from using fossils to renewable energy, and the benefits surrounding solar energy.

2.1.1 Push for Renewable Energy

Wood and other biomasses were once the main source of energy. Then with the introduction of the Industrial Revolution fossil fuels became the sought after source of energy. Due to the finite supply of both biomasses and fossil fuels and the growing demand for energy, there is motivation to identify reliable alternative sources. However, transitioning from fossil fuels can be a challenge since our infrastructure developed around them being the main source of energy. Thus, there must be economic motivation to move away from fossil fuels, which requires decreasing the production costs and expanding the market of the renewable energy industry. Another challenge is that as more countries develop, the demand for energy increases and fossil fuels are commonly used in several different types of energy sectors. In 2017, the Lawrence Livermore National Laboratory presented an energy consumption flow chart, estimating the amount of energy used by the US in different sectors. Petroleum was the largest energy provider for the transportation sector, providing 25.9 Quads (1 quad = 1 quadrillion btus) of energy out the the total 28.1 Quads used for transportation. Additionally, petroleum and natural gas provided over 70%, 18.22 Quads together out of 25.2 Quads, of the energy to the industrial sector. Coal and natural gases provided over half, 22.24 Quads out of 37.2, energy to the electricity generation sector. Finally, natural gases provide a large amount of energy to the commercial and residential sectors [2].

It takes thousands of years for fossil fuels to form and humans are consuming fossil fuels at a faster rate than natural reserves can be replenished. According to BP's Statistical Review of World Energy in 2016 and the World Resource Institute, there is about 115 years left in coal production and about 50 years of oil and natural gases if no new reserves are found and the rate of production stays constant [4]. It is estimated that there will be a huge drop in possible production of gas and oil by 2030, which requires more immediate solutions [3].

With the depletion of fossil fuels there is the issue of increasing demand. A study published by BP in June 2018 stated the use of coal worldwide from 1965 to 2016 has risen from 16,322 TWh consumed to 44,015 TWh. Similarly, oil and gas consumption has increased from 17,740 TWh and 6,823 TWh to 51,384 TWh and 37,264 TWh per year respectively. The global average per capita of energy consumption has also increased. From 1970 to 2014, the average consumption of fossil fuels per capita globally increased about 45% [5]. According to a report completed in 2013 by the U.S. Energy Information Administration, it is forecasted that the world energy consumption will likely increase about 56% from 2010 to 2040 [6].

While depletion and increased fossil fuel demands are of major concern, fossil fuels also produce greenhouse pollution and environmental problems. Coal is one of the largest producers of CO_2 and greenhouse emissions that have immense environmental impacts [7]. Renewable energy is a viable alternative to current fossil fuel energy sources. There are several reasons why renewable sources of energy are beneficial socially, environmentally, and economically. The main reason for renewable energy is that it reduces the amount of greenhouse gases that are emitted into the atmosphere. Once these greenhouse gases are released they have been noted to stay in the atmosphere for extended periods of time which has been correlated to accelerating climate change [8]. The finite availability of fossil fuels and the environmental hazard that they cause drives the search for renewable sources of energy. Another reason is that for the production of fossil fuels consumes large amounts of water and in countries with water scarcities, providing enough energy could be a challenge. Renewable energy can address this issue since it uses less water in comparison. A third reason is that renewable energy can provide energy security for countries that struggle to meet energy demands with fossil fuel. Finally, it can provide energy diversification and new sources of employment [3].

2.1.2 Benefits of Solar Energy

Solar energy has the potential of meeting the world's energy needs. This technology converts the energy from the sun into electricity which can be stored and distributed. Solar energy is readily available across the globe because it is sourced from the sun. The sun is considered to produce about a constant amount of power at 6.33×10^7 W/m^2. The sun's rays produce an average radiation intensity that hits the Earth's atmosphere with a 7% change depending on how close the Earth is to the Sun. This radiation intensity is called the solar constant, I_{sc}, and is the yearly average is 1367 W/m^2. However, only about half of the Earth faces the Sun at a time and due to the fact that the Earth is a sphere, the I_{sc} gets divided by 4, half for each circumstance, making I_{sc} equal about 340 W/m^2. When the radiation reaches the Earth, about 70% of it gets absorbed by the Earth so the amount of energy that is actually available is about 238 W/m^2 per day [30]. The available land United States is about 9.8×10^{12} m^2 [31.1] meaning that the just with the land of the United States alone, it has receives about 2.3×10^{15}

Watts per day of energy from the sun. In 2017, the United States consumed approximately 97.7 quadrillion (97,728,000,000,000,000) Btu [50].

Additionally, solar energy has the potential to be more economically viable than fossil fuels. Solar photovoltaic cells have become more commercially affordable from a module or a cell costing $100/Watt in 1976 to it costing $0.10/Watt in 2014. Solar energy is also a low-carbon emission energy source which would reduce the pollution caused by fossil fuels [10]. In the United States, solar energy is a part of several different sectors, commercial, industrial, education, military, and residential, and it has provided over 250,000 jobs since 2017 [49]. Solar energy has helped many business secure their own energy security by eliminating their dependence on large energy companies. By switching to solar energy, homeowners and businesses can save on electricity, receive tax credit and rebates, and sell surplus electricity. These incentives from the U.S. government help promote solar energy as an affordable and environmentally positive change [11].

2.2 Silicon Solar Cells

In this section, silicon-based solar cells and its shortcomings are introduced. Currently, silicon-based solar cells are the most commercially available solar cell technology.

2.2.1 Current Technology

Silicon is a popular semiconductor material for photovoltaic (PV) solar cells due to its availability and environmentally safe characteristics. Approximately 26% of the Earth's crust, by mass, is comprised by silicon and the use of silicon has reduced pollution and strain on natural resources (Green, 2009). Crystalline silicon PV solar cells are the leading commercialized solar technology. In 2008, these cells contributed to 90% of the world's PV solar cell production (Saga, 2010). Silicon photovoltaics exist in two forms: monocrystalline and polycrystalline (Solar energy technology basics, 2013). Mono and polycrystalline solar cells are displayed in Figure 1 alongside a generic silicon solar cell cross-section. (Saga, 2010). The first silicon solar cell, created by Russell Ohl in 1941, had a PCE of 1% (Green, 2009). Since then, major technological developments have managed to drastically increase the PCE to 25% for monocrystalline cells (Green, 2009), (Solar energy technology basics, 2013). This high PCE has been achieved in a laboratory setting, but has yet to be reached in industrial cells. Solar cells produced in industry remain at an efficiency of 22.5% (Aggarwal, 2018). An additional benefit to this developing technology is that it has little long term degradation. Crystalline silicon solar cells' stability and reliability allow for a lifetime of 25+ years (Solar energy technology basics, 2013). Thus, allowing a solar panel to generate 14-20 times its initial production energy investment [23]. While silicon based PV solar cells prove to be efficient, dependable, and stable there are production challenges that limit the expansion of the solar industry.

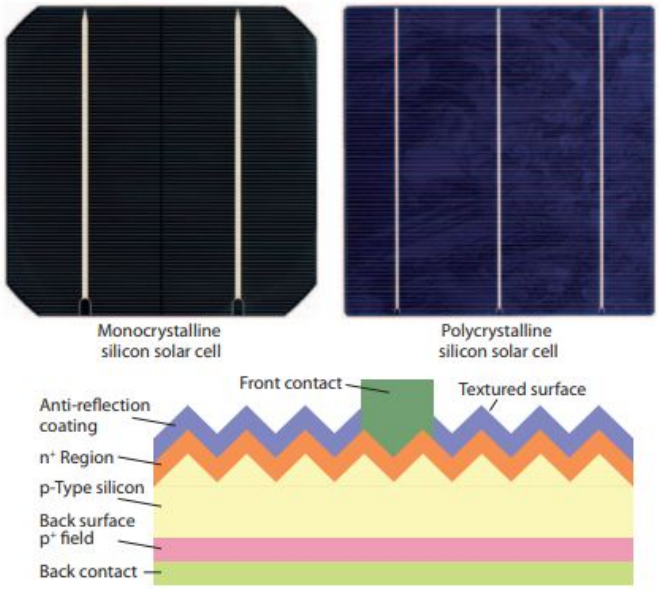

Figure 1. Typical mono- and polycrystalline silicon solar cells (upper), and simplified cross-section of a commercial monocrystalline silicon solar cell (lower) (© 2010 Sharp).

Figure 1. A depiction of the typical mono and polycrystalline solar cells

2.2.2 Shortcomings

While crystalline silicon PV solar cells dominate the global solar market, the high cost of production needs to be addressed in order for solar energy to be competitive with coal and nuclear energy. High-purity crystalline silicon substrates are very expensive due to the complex processing required to create the silicon crystals. It costs t approximately $2.58/W to produce a crystalline silicon solar cell; a mass production cost of less than $1/W needs to be achieved in order to grid parity with coal and nuclear energy (Saga, 2010) [22]. Decreasing the thickness of the silicon layer is a potential method for decreasing material consumption and production cost, but as the thickness decreases so does the cell's efficiency [22]. A potential technology to combat the production costs associated with silicon solar cells is thin-film perovskite solar cells [23]. These solar cells require less material and processing, making them more cost effective. Various semiconductor materials in perovskite solar cells have been researched which demonstrate promise for being competitive with silicon solar cells.

2.3 Lead-Based Perovskite

While research is being conducted into various materials that can act as the semiconductor layer in perovskite solar cells, the top performing material thus far is methylammonium lead iodide (MAPbI3). Lead-based perovskite solar cells and its downfalls are discussed in the following section.

2.3.1 Current Technology

Methylammonium lead iodide (MAPbI3) thin-film perovskite solar cells demonstrate the potential of perovskite cells outperforming silicon solar cells. Their desirable optoelectronic properties, such as high carrier diffusion length, optimal band gap (~1.6 eV), and strong absorption, result in a PCE of approximately 20% [23, 25]. This efficiency is comparable to that of industry level silicon solar cells but can be achieved at much lower production costs [23].

2.3.2 Shortcomings

Although $MAPbI_3$ perovskite solar cells compete with the efficiency level and production costs of silicon solar cells, their instability and toxicity are major concerns. Reports have found that UV light exposure decreases their stability and leads to reactions between the TiO_2 hole transport layer and the perovskite layer [23]. Additionally, the crystal structure of $MAPbI_3$ is sensitive to temperature changes where active layer damage was observed as the cell was subjected to increased temperatures [23]. During operation, solar cells will be exposed to increasing temperatures. Furthermore, irreversible degradation of perovskite solar cells is caused by moisture resulting in the formation of PbI_2. This leeches toxic lead into the environment and water sources [23].For human beings, lead exposure can result in a variety of health problems including cancer and neurological damage. Perovskite solar cells are a promising solar technology, but semiconductors with increased stability and nontoxic characteristics are needed.

2.4 Bismuth Triiodide Potential

The following section provides pertinent information regarding the primary material of focus in our research, BiI_3. Its benefits as a material for the active layer of a solar cell is provided as well the current technology that surrounds it and its limitations.

2.4.1 Benefits

Bismuth triiodide (BiI_3) has the following benefits as a PV material: it is non-toxic, has an ideal band gap, is easily processed by multiple methods, and is not a rare earth metal. As stated previously, lead- and cadmium-containing thin-film solar cells have an efficiency that is competitive with silicon solar cells. Bismuth-based materials are a non-toxic alternative that also have the potential of creating high power conversion efficiency (PCE) thin-film solar cells. Generally, PV materials have an ideal band gap of approximately 1.4 eV [15]. As can be seen in the figure below, BiI_3 falls within the ideal band gap range for PV materials.

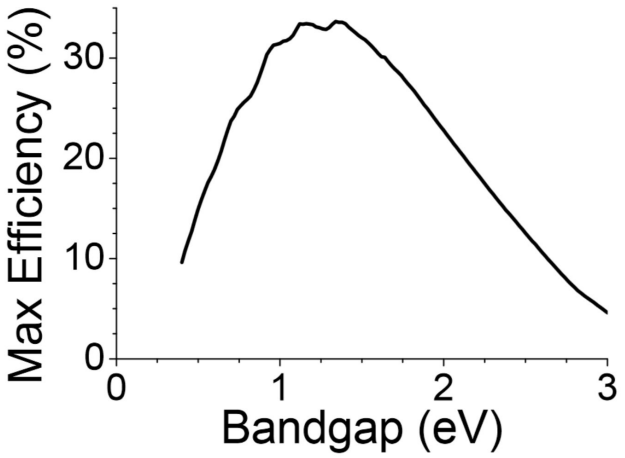

Figure 2. Shockley-Queisser limit graph

BiI_3 has an indirect band gap which occurs around 1.7 eV [16]. An indirect band gap is when the momentum of the valence band and conduction band are not equal. In other words, electron-hole pairs are not as easily made in indirect band gap compared to direct band gaps. This still results in a maximum efficiency of over 20%, making it a favorable material for further research. Additionally, a band gap of approximately 1.8 eV is ideal for BiI_3 in order to be used in tandem with silicon solar cells [29]. This would avoid the need of having to replace all the silicon solar cells that are currently used since BiI_3 would be versatile enough to work alongside silicon or act as a stand alone material. The silicon cell will absorb more of the red and infrared radiation, whereas the BiI_3 would absorb the UV, blue, and green radiation.

Furthermore, BiI_3 can easily be processed by a variety of methods including solution processing and evaporation techniques [12, 13]. In solution processing, which typically involves spin-coating, a solution of BiI_3 is dropped onto the substrate and is then spun for a set amount of time at a set rotations per minute (rpm). This deposits a thin film of solution-solvent complexes which is subsequently annealed, around 125 ^{o}C, to drive out remaining solvent and crystalize the BiI_3. Alternatively, BiI_3 will readily evaporate under vacuum conditions at temperatures around 200 ^{o}C; evaporation is a low-temperature processing method. BiI_3's high solubility and low-temperature-processing contribute to its overall simplicity compared to processing silicon solar cells. Both of these methods fabricate BiI_3 thin films with different crystal structures and orientations. Thus, there is plenty of potential for bismuth-based solar cell research.

In the search for new PV materials to replace silicon that can be easily processed, one major factor is material abundance. Establishing a solar cell process in which the use of significant amounts of extremely rare elements is needed is not a viable solution. Bismuth, while not as nearly as abundant as silicon, is not a significantly rare element. The chart below depicts atomic abundances in relation to silicon. Bismuth, with a atomic number of 83, is around 10^{-1} on the scale meaning that for every 1 million atoms of silicon, there is about 100,000 atoms of bismuth. If bismuth solar cell efficiencies can be significantly improved, the amount of bismuth

needed per unit of energy converted would most likely be less than the amount of silicon currently used per unit of energy converted, even though there is less bismuth available than silicon.

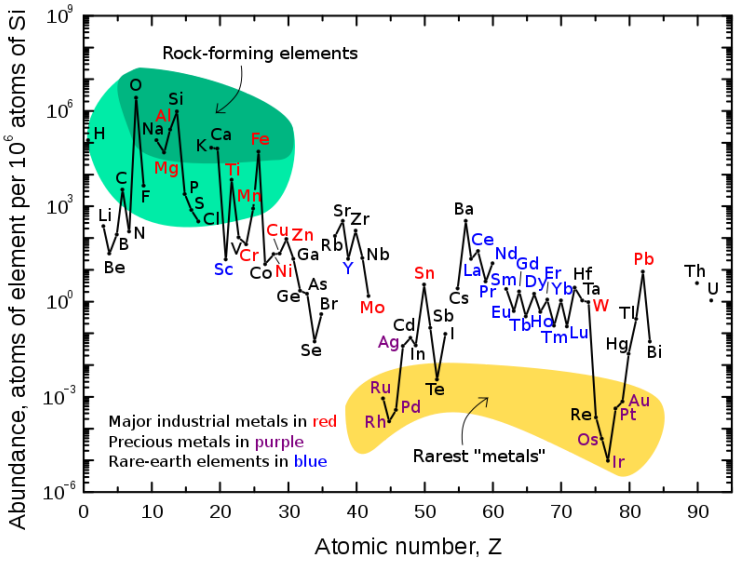

Figure 3. Elemental abundance graph

2.4.2 Current Technology

The success of solar energy depends greatly on the ability to develop new and innovative technologies. So far, thin-film solar cells show promise in their ability of being easily processed at lower temperatures than standard silicon solar cells. However, the only thin-film solar cells that have shown PCEs on par with silicon solar cells either contain toxic chemicals (such as lead in MBI or cadmium in CdTe and CIGS), are expensive to manufacture (CIGS and CdTe solar cells), or contain rare metals (such as tellurium in CdTe) [17, 26, 27]. MBI, CdTe, and Cu (In,Ga) Se_2 (CIGS) solar cells all have efficiencies of around 20%, similar to silicon solar cells.

BiI_3 has shown potential as both an absorbing layer in thin-film solar cells [12, 13] and as a hole transport layer in organic solar cells [14]. In the majority of research done so far, BiI_3 films are fabricated via solution processing techniques for use in thin-film solar cells. BiI_3 behaves as the light absorbing layer in which electrons are excited from the valence band to the conduction band. Ideally, these excited electrons and the resulting 'holes', net positive charge due to the absence of an electron, will travel through the BiI_3 layer towards the electron transport layer and the hole transport layer, respectively. This charge is then carried out of the material through the conductive contact and used as an electricity source.

2.4.3 Shortcomings

While bismuth easily dissolves in many solvents, many problems arise with solution processing layers around BiI_3. For example, if the hole transport layer material is dissolved in a solvent which BiI_3 is also soluble in, then when the cell goes through spin-coating for the HTL solution, it will dissolve the BiI_3 layer. This can be overcome by thermally evaporating the hole transport layer so that there is no solvent to contact the BiI_3 in the first place. Additionally, BiI_3 grows as a two-dimensional anisotropic crystal making it a challenge to develop into a film that can efficiently transport charges without having to cross as many grain boundaries. However, BiI_3's largest shortcoming is its extremely low PCE. The highest recorded PCE is approximately 1% [20, 28]. In order to become a competitive PV material, its PCE must be improved significantly.

Chapter 3: Background

In this chapter, an overview of thin-film solar cells, BiI_3, and the hole transport layer (HTL) is presented. First, the importance, liminations, and fabrication methods of thin-film solar cells is detailed. Then, the role of the active layer and crystal orientation is described as well as the crystal structure of BiI_3. To conclude, the importance of the HTL, and the materials that can be used, are detailed.

3.1 Concept Behind Thin-Film Solar Cells

In this section, the idea behind thin-film solar cells is presented. Information about its overall assembly and manufacturability are addressed.

3.1.1 Thin-Film Solar Cells

Thin-film solar cells aim to fill the need of cheap, easily producible solar cells. The price reduction potential of silicon solar cells is extremely limited, making them difficult to become competitive with the other fuel sources [34]. Thin films for photovoltaic (PV) applications can be produced by various methods such as: spin-coating, vapor transport, and sublimation. Additionally, different post-deposition treatments can be performed such as: ambient thermal annealing, solvent-vapor annealing, and petri dish annealing [35]. Thin-film solar cells are typically assembled in the following order: FTO contact / electron transport layer (ETL) / absorber layer / hole transport layer (HTL) / Au contact. Ideally, the absorber layer should have a band gap within the Shockley-Queisser limit, as described earlier, so that it can efficiently absorb sunlight and excite electrons from the valence band to the conducting band. An excited electron carries with it a net negative charge leaving behind a net positive charge, a hole. The electron

will travel towards the electron transport layer while the hole will travel to the hole transport layer. At both, the absorber-HTL and absorber-ETL interfaces, there is a small electric field region which pulls either the electrons or holes to their respective transport layer once they diffuse far enough through the absorber. The sandwich of ETL / absorber layer / HTL aims to achieve this function where excited electrons from the absorber layer and its resulting hole are diffuse around in the absorber material until they reach their respective space charge region and are pulled to the transport layers by the electric field. Utilizing this phenomenon, thin-film solar cells can be fabricated. However, the challenge now lies in finding a material which is able to not only efficiently excite electrons, but also be fabricated in such a way that its interactions with the ETL and HTL is effective and does not hinder charge transport. BiI_3 has the ideal band gap to effectively excite electrons and is easily processable by multiple methods. BiI_3 dissolves and sublimes easily, while not requiring high temperatures to be processed.

3.2 Potential Avenues for BiI_3's Development

This section highlights the particular avenues have been taken and issues that must be addressed in order to improve the development of BiI_3.

3.2.1 BiI_3's Development

From the various researches that has been done on BiI_3, particularly in the past 5 to 10 years, it appears that the material has the potential to be an ideal absorber material to continue exploring (Patil & Talele 2012; Devidas et al. 2014; Lehner et al. 2015; Brandt et al. 2016; Hamdeh et al. 2016; Kulkarni et al. 2018; Tiwari et al. 2018). However, there are particular areas that need to be improved in order for the material to become a competitive PV material. First, fabrication techniques must be addressed. Thus far, most of the research into BiI_3 has been with the use of solution-processing, but only small breakthroughs have been made with this method (Hamdeh et al. 2016; Kulkarni et al. 2018). As mentioned previously in Chapter 2, the highest PCE achieved using BiI_3 was about 1% (Hamdeh et al. 2016). BiI_3 can also be easily processed by evaporation and sublimation, but as of today, little research has been done in fabricating BiI_3 solar cells through these methods. In fact there evidence that through evaporation, there's the potential of controlling the crystal orientation of BiI_3 (Brandt et al.).

Additionally, solvent-vapor annealing and drop-coating are other effective processing methods for thin-film PV materials. In solvent-vapor annealing, a material is annealed in a closed system alongside drops of a solvent. During annealing, the atmosphere is saturated with vapor from the solvent so that when BiI_3-DMF complexes break apart and evaporate, they do not entirely leave the system entirely. Deposited BiI_3 is forced to remain within the solvent in the thin film. Given time, the BiI_3 can recrystalize and grow larger (Kulkarni et al. 2018). On the other hand, drop-coating involves dropping a solution or liquid onto the deposited film while it is being spin-coated. The idea behind this method is that the BiI_3 will have a low enough solubility in the

dropped liquid or solution,toluene or nearly saturated BiI_3 solution in DMF, so that the BiI_3 only partially dissolves. Thus when BiI_3 re-crystallizes, a more uniform film will be formed (Kara et al. 2016). Typically, BiI_3 forms a highly non-uniform film. Dropping toluene, a nonpolar solvent, improved efficiency and reproducibility in MBI cells in Kara et al.'s work. An improved film quality will allow for better interfacial interactions with the ETL and HTL layers and less grain boundaries, i.e. locations for charges to concentrate and make charge transport more difficult. All in all there is great potential for BiI_3 as an absorber layer in thin film solar cells and research should continue to explore new material combinations and processing methods.

3.3 Importance of Active Layer Crystal Orientation

The processes used to deposit the active layer onto a solar cell, and the crystal orientation that in turn is produced during such process, plays an important role in the effectiveness of a solar cell. This section outlines the crystal structure of BiI_3 and the methods that have been used to deposit the active layer.

3.3.1 Crystal Structure of BiI_3

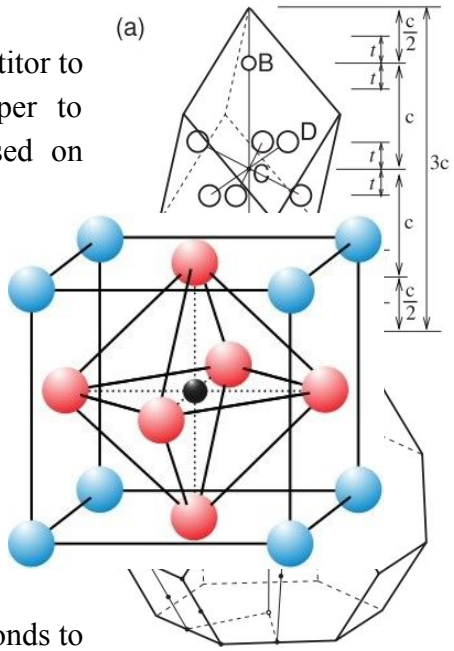

Thin-film solar cells are emerging as a potential competitor to crystalline-silicon solar cells as they are easier and cheaper to produce. Primarily thin-film solar cells research has focused on materials with the perovskite crystal structure, (seen Figure). The perovskite crystal structure allows for a unique set of properties, such as ferroelectricity and superconductivity, making it the material for the active layer within solar cells. While the active layer material in focus, BiI_3 , does not have the typical perovskite structure, it exhibits properties similar to that of conventional perovskite materials and is thus deemed "perovskite-like" [32]. Theoretical and experimental data demonstrates BiI_3 as having suitable band gap, electron mobility, and potential "defect-tolerance" for typical thin-film solar cells [35]. Perovskite compounds contain an anion that bonds to two cations in the chemical formula ABX3, as seen in Figure [31]. BiI_3 has two types of crystal structures: rhombohedral and hexagonal, both structures are demonstrated in Figure (a and b) [36]. According to Brandt et al, the success of BiI_3 as a semiconductor stems from its layered, two-dimensional, hexagonal structure.

3.3.2 Optimizing and Controlling Crystal Orientation

It has already been proven that it is possible to obtain PCEs as high as 20% for some three-dimensional perovskite active layers. However, the stability of the layer still remains a challenger. A possible solution for increasing the environmental and photo-stability of the cell would be by processing two-dimensional perovskite crystals. In terms of stability, two-dimensional perovskite crystals outperform three-dimensional perovskite crystals, , but they only reach an efficiency of 4.73%. Tsai and Mohite were able to overcome this challenge by producing nearly single crystalline thin films for efficient charge transport, resulting in a PCE of 12.52% [37]. They attributed the increase in charge transport to the perpendicular orientation of the semiconductor crystals relative to the substrate. The active layer in this study was of the methylammonium lead iodide family, but control of BiI_3 crystals could prove to have similar increases in stability and PCE [37]. Research has showed a variety of methods for processing vertical crystals. Tsai and Mohite utilized a hot-casting method where the FTO substrate was heated from 30 °C to 150 °C on a hot plate for 10 minutes. The solution was also heated at 70 °C and stirred for 30 minutes before spin-coating at 5000 rpm for 20 seconds onto the hot substrate. At the completion of spin-coating the sample was quickly removed [37]. An additional method, specifically for BiI_3, showing that solution-processed films deposited on glass at temperatures of around 110 °C oriented more vertically in relation to the substrate [35]. Finally, for BiI_3 in X-Ray applications, it was found that vertical physical vapor deposition of BiI_3 followed by crystal growing at approximately 150 °C for 3 days resulted in microcrystals growing along their c-axis perpendicular to the glass substrate [38]. However, little research literature has been found on the vapor deposition of vertically oriented crystals for solar cell applications which will be the primary focus of this research as outlined in Chapter 4.

3.4 Potential Materials for Hole Transport Layers

The following section provides information regarding the need and usage of a hole transport layer (HTL) in a solar cell. Essential information of how the HTL is characterized and the different types of hole transport materials (HTMs) that exist are introduced, including the HTMs that are of focused in our research and how they are going to be deposited.

3.4.1 Organic vs. Inorganic Hole Transport Layers

3.4.1 Importance of Hole Transport Layer

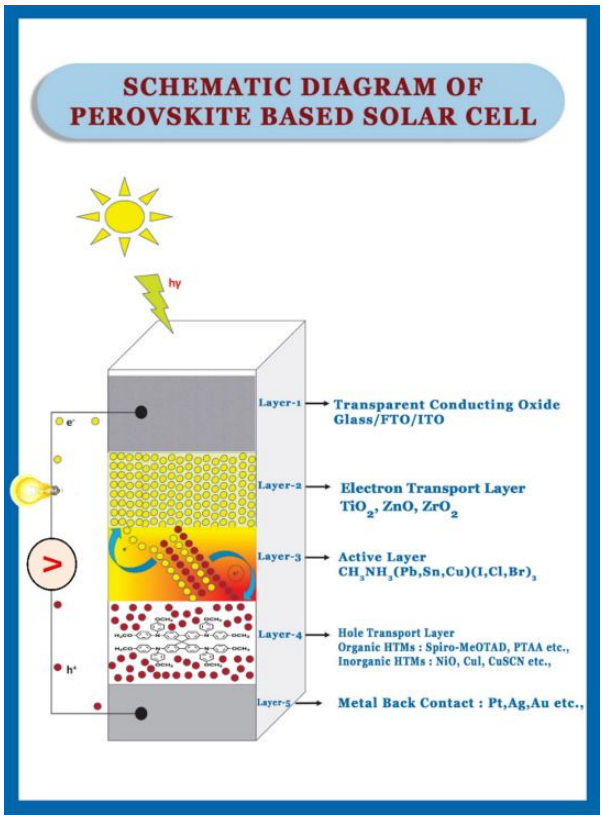

In a solar cell, the HTL is used to extract holes from the absorber layer and to act as a protective layer between the metal back and the active layer. It has also been known that the HTL can improve the charge carrier collection efficiency. Additionally, the HTL replaces the use of liquid electrolyte as a solid electrolyte in the cell [29]. Deciding on which HTMs to use when assembling a solar cell generally depends on the materials that were used for the other layers and how it will react with them. For example, depending on the type of HTM, it can have different energy levels. The same goes for the electron transport layer. When the energy levels of both layers are subtracted from one another, it will give you the theoretical maximum voltage that can be obtained.As seen in Figure X, the energy level of TiO2, the electron transport layer that is used in our lab and for our project, is 4.3. The three HTM that can be used is P3HT, CuI, and CuSCN, with respective energy levels of 5.0, 5.1, and 5.3. With this information, CuSCN should have the highest voltage. A better HTM would be one of the polymer materials such as CPB but those are extremely expensive [46].

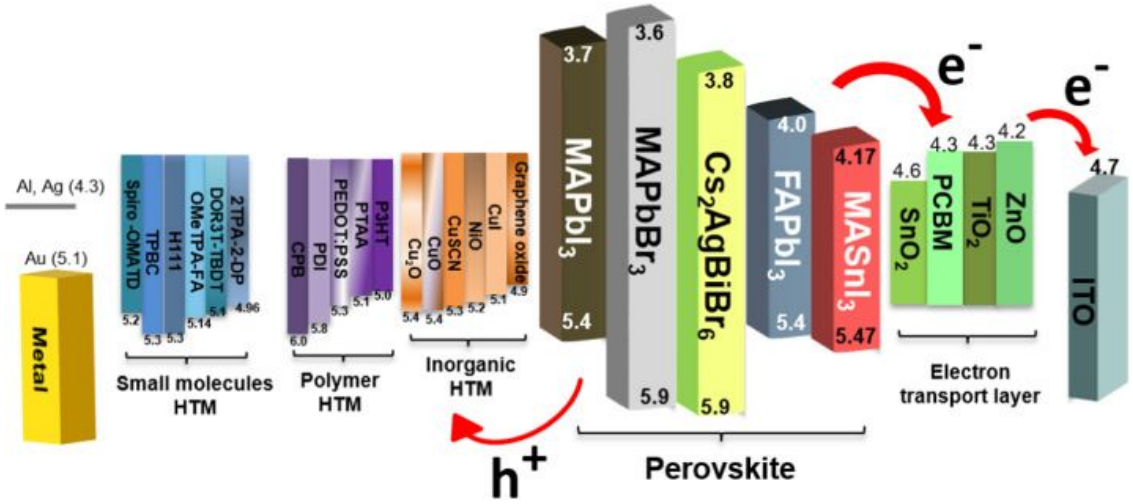

Figure 4. A depiction of the ionization energy for different materials [46]

To be the right HTM for the HTL, the material also needs to be able to have the proper energy levels, high conductivity and charge mobility, high thermal and photochemical stability, good solubility, good film-forming properties, be of low cost, and have easy manufacturability. One of the most important characteristics that the HTM must have is hydrophobic properties to protect the active layer from moisture exposure. Depending on the quality of the HTL, the perovskite will be protected according to from air and diffusion from elements in the absorber [28.1].

There are various organic HTMs already on the market that have proven to have a high open circuit voltage and can reach high PCEs. The main issues with these types of organic materials are the fact that industrial development and market potential have been restricted due to their cost and instability when exposed to water, heat, and light. The most common type of organic HTMs are P_3HT and PEDOT: PSS. On the other hand, inorganic hole transport materials are less expensive and more stable. Possible inorganic HTMs have been identified as NiO, Cu_2O, CuO, CuCrO2, CuGaO2, and CuI. Although inorganic materials are more stable, their efficiencies are low. However, there is a larger market push for inorganic HTMs than their organic counterparts [27.1]. In the past few years, inorganic HTMs have been recorded as having an increased PCE, but the limited choices of deposition techniques are another setback that needs to be overcome [28.1].

3.4.2 Hole Transport Materials of Focus

3.4.2.1 CuI and CuSCN

As mentioned previously, inorganic HTMs have shown the potential of becoming promising materials for the HTL. Their stability and recorded improvement in increasing the PCE of solar cells are just a few of the characteristics that makes attractive in the market. Their high hole mobility, wider band gap, and high conductivity also contribute to their rise as potential HTMs. However, at the same time inorganic HTMs are sensitive to moisture and oxygen, two things that hinder their potential as materials for the HTL.

In our research, we're going to focus on copper-based inorganic HTMs, specifically CuI and CuSCN. Some of the benefits of using copper-based inorganic HTMs are their low cost synthesizing methods (solution-based process), wide band gap, stability, and high conductivity [30]. CuI has been proven to achieve relatively high PCE depending on the texture of the perovskite film. In 2015, Chen et al. synthesized CuI as the HTM in perovskite solar cell instead of PEDOT:PSS and noticed that cell's performance and stability increased [30]. In a study conducted by Ye et al., a PCE of 16.6% was recorded by a perovskite solar cell with CuSCN as a HTM [43]. Another study shows that CuSCN when deposited through the solution on an indium doped tin oxide substrate, ITO, created a layer proves that copper can make a porous layer that could be an advantage to working on efficiency and creating a better HTL. However, a

disadvantage that was discovered was that if the layer was too thick, the efficiency of the HTL would decrease [39.1]. Both, CuI and CuSCN, have shown the potential of being promising materials for the HTL, however, further research on their full capabilities and limitations need to be conducted.

3.4.2.2 Deposition Methods

CuI can be deposited in various ways onto a solar cell, but first it needs to be mixed into a solution. Once a solution, CuI can be spin-coated onto a solar cell and then heat treated for several hours [41]. A study conducted in 2014 used the drop casting method to deposit CuI onto the solar cell. Other ways of preparing the HTL using CuI are through chemical bath deposition and spray coating. For our research, CuI was deposited through thermal evaporation. By controlling the evaporation rate, the CuI film growth was controlled. To go about thermal evaporating CuI, a study was done where the film was deposited onto a quartz substrate. The substrate was placed into a chamber with a boat that contained pure CuI (99.9%) powder. The chamber's pressure dropped to 5 x 10^{-5} mbar with a current of 80 A running through the substrate. The boat and the substrate maintained a distance of 10 cm, but the substrate will also be rotated at a speed of 10 rpm keeping the same distance to create a more uniform film. This method shows an improvement of properties in the HTL that is correlated to the growth parameters set in this study [42]. Our group translated this evaporation technique into a close-spaced sublimation method. The CuI powder was placed into the boat with the substrate face down and the temperature was incrementally increased until the CuI began evaporating. This deposited CuI directly onto the substrate.

CuSCN has previously been deposited through electrochemical deposition, successive ionic layer adsorption and reaction, and chemical bath deposition [44]. Similarly to CuI, CuSCN needs to first become a solution before being deposited. For our research, CuSCN (40 mg) was dissolved in diethyl sulfide (1 mL) and stirred on a hot plate (60 ^{o}C, 800 rpm) for at least two hours. After stirring, it was filtered using a 0.2 micrometer filter tip. From here, 35 microliters of the filtered solution was dropped onto the already-spinning substrate (4500 rpm for 35 seconds). Typically, the diethyl sulfide would dissolve the BiI_3, however in this process, the diethyl sulfide is saturated with CuSCN. Specific to this spin-coating procedure, the substrate is given 5 seconds to reach its maximum rotational velocity, and then the 365 microliters of CuSCN solution are uniformly dropped over a period of 2-3 seconds. This allows for minimal solvent-BiI_3 contact and deposition of the CuSCN hole transport layer. There is no annealing procedure for this layer.

Chapter 4: Objectives and Hypothesis

The following section provides a more detailed description of our objectives and hypothesis. First, the objectives are introduced followed by a brief description on why achieving them is important. This section ends with our hypothesis.

4.1 Controlling the Orientation of BiI_3 Crystals

Identify if the orientation of BiI_3 crystals can be control through close-spaced sublimation (CSS).

The purpose of this objective is to determine if the orientation of BiI_3 crystals can be controlled to be vertical or horizontal through close-space sublimation (CSS). However, first we must establish a procedure for evaporating BiI_3 through CSS. Currently, there's not much research, and literature, demonstrating how to add BiI_3 to thin-film solar cells using CSS, so a functioning solar cell needs to be assembled. By being able to control the crystal orientation, the efficiency of BiI_3 thin-film solar cells can also be control. Additionally, identifying how to control the crystal orientation of BiI_3 can provide a better understanding on how the crystal orientation has an effect on the results of various applications.

4.2 Identify which Crystal Orientation is Better

Determine which BiI_3 crystal orientation will allow for easier charge transport and increased efficiency.

Once knowing how to control the crystal orientation, BiI_3 thin-film solar cells can be created with the different crystal orientation to determine which will allow for easier charge transport and an increase in efficiency. To characterize our samples, the methods that used were SEM, optical imaging, light absorption test, quantum efficiency analysis, and performance testing. THz spectroscopy, photoluminescence, XRD, and Hall Effect are other methods that can be used to characterize solar cells.

4.3 Improving the Overall Cell Performance

Improving the overall cell performance through techniques such such as annealing and modifying the hole transport layer.

We switched the hole transport layer (HTL), P3HT, that was being used in the lab to CuI and then to CuSCN. By switching from P3HT, an organic HTL material, to CuI and CuSCN, both inorganic HTL materials, the HTL can potentially become more stable and aid in increasing

the efficiency by more efficient charge extraction. CuI was deposited using CSS while CuSCN was deposited using solution processing.

We also added annealing as a step between depositing the BiI3 and the HTL. Initially, we started with just annealing the samples on a hot plate for an hours. Later, we tried the effects of annealing the samples in a closed chamber with Iodine.

4.4 Hypothesis

We are working on controlling the crystal orientation of BiI_3 as it gets deposited on the sample. Once we have developed a method of controlling the crystal orientation, we plan to test the different orientations to see which will provide better results. We have hypothesized that vertical crystals will provide the easiest path for charges, thus increasing the solar cell efficiency as opposed to horizontal crystals. However, we believe that the horizontal crystals will interface better with the adjacent hole transport layer. The horizontal and vertical orientations will be analyzed and compared using SEM, absorbance measurements, and solar performance testing.

Chapter 5: Experiment Designs and Testing

In this chapter we provide a breakdown of how each sample was prepared. First, the initial steps towards preparing the sample is described, followed by the deposition of the hole transport layer (HTL). Then, the process used to evaporate and deposit BiI_3 is described, including the post-evaporation methods experimented with. Next, an overview on how CuI and CuSCN were deposited is provided and lastly, this chapter ends with how the deposition of the gold layer is conducted.

5.1 Preparing Substrate

In this section, the first step towards preparing the samples is briefly detailed. The cutting and cleaning of the samples are essential steps in the process since a well clean sample would ensure the uniformity of the hole transport layer (TiO_2). Thus, resulting in a cell with a promising PCE.

5.1.1 Cutting and Cleaning

The first step towards preparing each sample involves cutting fluorine doped tin oxide (FTO)-Glass sheets into 2 cm x 2.5 cm rectangles. The FTO-Glass sheets can be marked with a marker for the measurements because during the cleaning process the marks will be erased. Once the desired amount of FTO-Glass rectangles is obtained, the conductive side of the samples is identified using a multimeter. Then, with the conductive side facing up the samples are placed in a plastic petri dish where they can be stored until the cleaning process can begin.

Next, to begin the cleaning process make sure that the conductive side of the samples is facing up when they are placed in a glass petri dish. Sonicate for 5 minutes the samples 3 times in 1:1:1 mixture of isopropyl alcohol, acetone, and DI water. Each time the sonication is complete, pour the old mixture in the appropriate waste bottle. Once the 3 runs are complete go over the samples with either acetone or ethanol with a Q-tip to completely erase any marker marks. Lastly, using only DI water sonicate the samples for 10 minutes and dry with compressed air and place the samples in a clean plastic petri dish until the hole transport layer (TiO_2) can be added. Make sure to store the samples with the conductive side facing up. Refer to Appendix A for a more detailed approach on the cutting and cleaning of the samples.

5.1.2 Adding the Electron Transport Layer (TiO_2)

One of the most important components of preparing a solar cell is adding the electron transport layer (ETL), in this case we will be using two solutions of different molar

concentrations of titanium oxide (TiO_2). Refer to Appendix B for the specific calculations on how create the two TiO_2 solutions and the order on how they will be deposited onto the samples. Before depositing the solutions onto the samples, use a piece of tape to cover a small section of the samples before each spin-coating section to ensure that there will be an FTO section exposed. If the next layer won't be added right after, make sure to store the samples in a clean plastic petri dish. Use parafilm tape to ensure that oxygen or moisture won't get in and then cover the petri dish with foil paper so the samples won't be exposed to light.

5.2 Procedures for Evaporating BiI_3

5.2.1 Close-Space Sublimation

To deposit BiI_3 onto our samples through close-space sublimation (CSS) we first had to design and build a testing site. In a lab designated area, we set up a vacuum, heating tape, quartz tube (chamber) with stand up holders, thermocouples, and rubber stoppers as the primary components of our design. Then, we used a metal rod, substrate holder, and wire to build the part that would hold our samples inside the quartz tube. Refer to *Figure 5* for reference on the design set up.

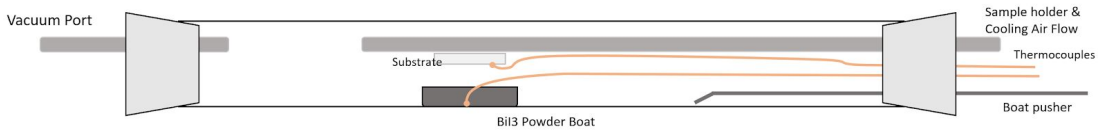

Figure 5. Diagram of Close-space Sublimation Set Up

In close-space sublimation, the temperatures and distance between the substrate and source greatly influence the film growth rate as well as the pressure and vapor composition within the chamber [47]. In our set up, BiI_3 powder was placed at the bottom of an evacuated chamber (quartz tube) while the substrate was held face-down towards the powder by the substrate holder. Thus, when the source reached the desired temperature, the boat containing BiI_3 powder would be pushed into the heating zone, and evaporate the BiI_3 would evaporate on top of the TiO_2 layer [48].

In order to control and maintain the substrate and source temperatures within the specific range for both vertical and horizontal crystals, we tried the following: flowing water through the substrate holder, flowing air through the substrate holder, and decreasing and increasing the voltage of the heating tape. After various runs, we determined that flowing water through the substrate holder was not a viable method since we couldn't control the temperature of the water and when it was introduced to the experiment, it would drastically decrease the source

temperature. On the other hand, flowing air allowed for much more precise control over the substrate temperature.

5.2.2 Annealing

After evaporating BiI_3 through CSS, we tried thermal annealing, iodine annealing, and solvent-vapor annealing methods on halves of some of our samples to determine if they would help with the uniformity or crystallization of the layer.

5.3 Adding the Hole Transport Layer

5.3.1 CuI

CuI was attempted using close-space sublimation where the substrate and CuI powder are under vacuum and the powder is heated up until it evaporates and deposits in a direct line-of-site PVD method onto the substrate. This was done at 450 ^{o}C for 30 minutes under a vacuum of approximately 200 mTorr.

5.3.2 CuSCN

CuSCN was deposited using spin-coating methods where the solution is dropped on an already-spinning substrate at 4500 rpm. The solution is dropped over a 2-3 second period and the substrate is then allowed to spin for 30 seconds. There is no annealing needed for this technique. The solution is made by dissolving 40 mg of CuSCN in diethyl sulfide, followed by subsequent hot plate stirring (60^{o}C for 2 hr at 800 rpm) and then filtered through 2 micron filter.

5.4 Adding the Gold Layer

The final step is to add gold, the other conductive besides FTO, contact to complete the circuit. This is done using thermal evaporation equipment. Pure gold wire is placed into a resistive heating coil, with the samples below. The samples are covered in foil masks that are cut out where the gold contacts should be deposited. The chamber is brought to extremely low vacuum and the gold is evaporated in a line-of-site PVD method directly onto the substrate. These samples are removed and the mask is taken off, resulting in the complete solar cell.

Chapter 6: Data Analysis

6.1 Close-space Sublimation of BiI_3

The major focus of our research into close-space sublimation of BiI_3 was to develop a procedure for control the crystal orientation. At high temperature differences, we expect vertical crystal orientation, and at low temperature differences we expect horizontal. However, 'high' and 'low' are subjective. Our group tracked each fabrication and filled out a chart showing source temperature of the x axis and substrate temperature on the y axis. Not all samples we fabricated actually fit on this chart, thus they are not all shown here. After SEM analysis, it was apparent that around approximately 55 ºC is the transition boundary for the horizontal and vertical orientation. The top right will produce vertical and the bottom left will produce horizontal. Source temperatures below 190 ºC will evaporate BiI_3 but not at a sufficient enough rate for a reasonable evaporation time.

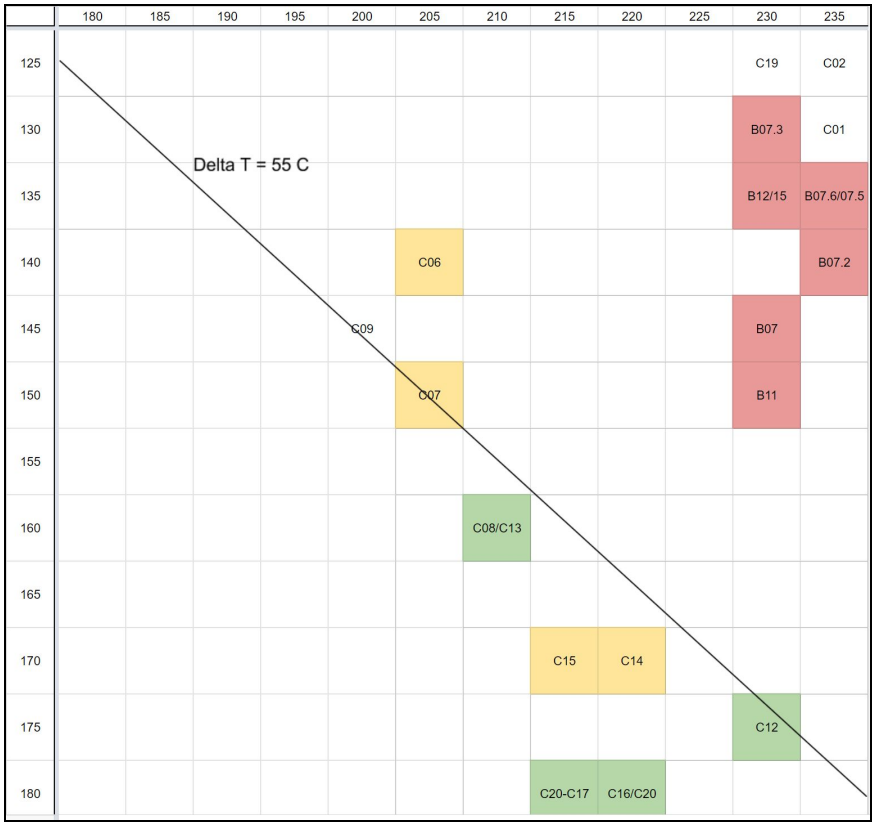

Figure 6. Matrix depiction of samples created through B and C term with source temperature on the x axis and substrate temperature on the y axis

To demonstrate the effect of temperature difference on the crystal orientation, the figure below displays the transition.

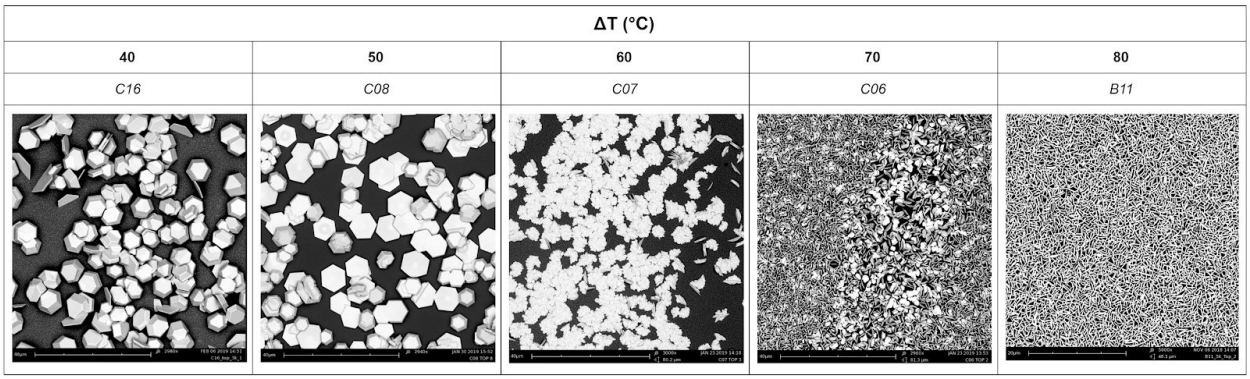

Figure 7. SEM pictures depicting the BiI_3 morphology with varying temperature difference

Shown above, it is clear that with a temperature difference of around 40 ^oC clearly results in horizontal orientation and a difference of around 80 ^oC results into uniformly vertical crystals. The intermediate temperature differences show mixed orientation, with 50 clearly favoring horizontal and 70 clearly favoring vertical.

One other major observation from these images is the substrate coverage. When vertical, there is a high density and coverage of the substrate. However, horizontal results in a lot of empty space on the substrate. Poor substrate coverage can often unintentionally result in short circuits in the full cell. If there are holes or empty spaces in the TiO_2 layer, when the gold is deposited it is possible for it to contact the FTO. This would results in a short circuit and effectively ruin the cell.

Vertical fabrication would routinely result in visibly uniform and dense films, as shown in the image below. However, horizontal evaporation would routinely result in scattered, sparkly, and poor coverage substrates. This could potentially be explained by BiI_3's tendency to prefer to bind with itself as opposed to the TiO_2. When there is high supersaturation (vertical), there are plenty of opportunities for nucleation sites, and these coordinated 2D crystals do not need to collectively bind to the TiO_2. However, with horizontal crystals, the entire face of the 2D crystal needs to bind to the TiO_2 surface. Thus, with a high enough substrate temperature during horizontal nucleation, there is enough energy to promote surface diffusion of the BiI_3 molecules where they would selectively move to and nucleate from the already growing crystal as opposed to creating a new nucleation site on TiO_2 and filling in the empty space. This also explains the high density of vertical crystals, because there are much fewer atoms per crystal in direct contact with TiO_2, allowing it to really fill in and nucleate. High supersaturation (high temperature difference) results in atoms preferentially binding to themselves and result in these vertical

nanostructures. Low supersaturation (low temperature difference) usually result in the vapor molecules preferentially binding to the substrate, and creating a flat film. In our case they do nucleate horizontally but they do not prefer to fully cover the substrate. Instead, the will grow outwards as well as grow thicker. Visually, this results in sparkly and scattered nucleation sites, which make it poor for use in solar cells.

6.2 Performance Testing Results

Up to this point, our group was only able to fully fabricate and test vertical cells. The horizontal samples have yet to come out sufficient enough to be made into a full cell.

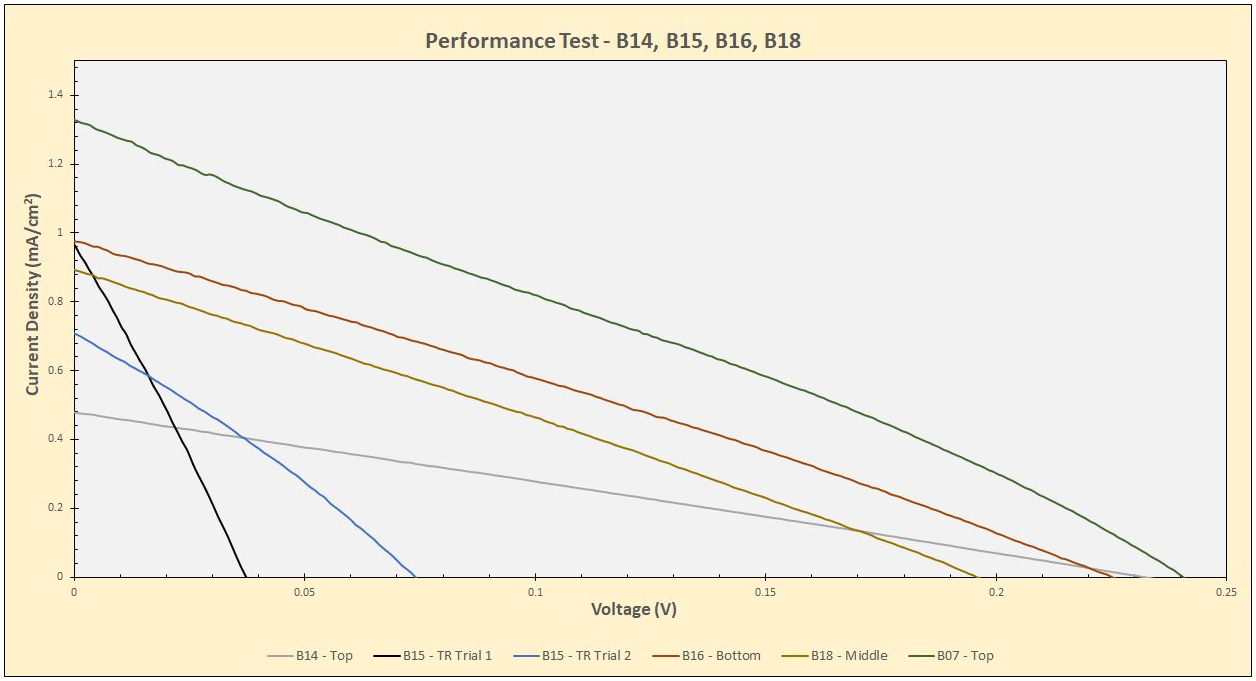

Figure 8. Performance test curves for samples B14, B15, B16, B18, B07

Above, performance tests for Samples B07, B14, B15, B16, and B18 are shown. This graph shows Current Density against Voltage, the defining performance curve for photovoltaic cells. The champion cell from these tests is the B07 cell, with an open circuit voltage of approximately 0.236 V and a short circuit current of about 1.32 mA/cm^2. Additionally, while its fill factor is not ideal at all, it does show small characteristics of the typical bended-line of a solar cell curve. B07 was fabricated with a source temperature fo about 230 ^{o}C and a substrate temperature of approximately 143 ^{o}C (~88 ^{o}C temperature difference), and was allowed to evaporate for 10 minutes at a pressure of approximately 250 mTorr.

While this cell provided the overall best efficiency, sample C04 resulted in the greatest open circuit voltage, as shown below. This cell had an open circuit voltage of approximately 0.243 V.

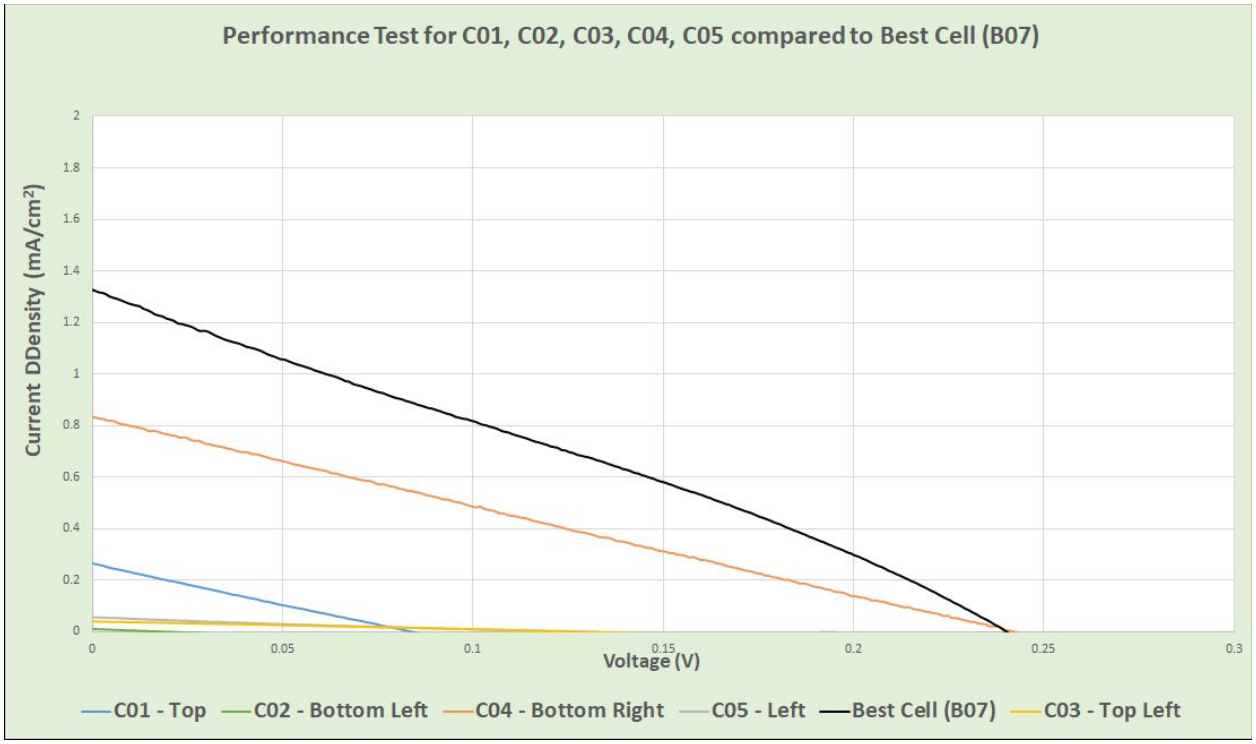

Figure 9. Performance test curves for C01, C02, C03, C04, C05, B07

6.3 Hole Transport Layer Development

While depositing CuI via CSS onto the BiI_3 thin film, our group ran into an issue. CuI has an evaporation point significantly higher than that of BiI_3. Thus, when evaporating CuI, the chamber exceeds BiI_3 evaporation temperature and evaporates the BiI_3 off of the substrate. After this realization, we pursued CuSCN via solution-processing instead.

6.3 Annealing Methods

6.3.1 Thermal Annealing

Our group attempted to use thermal annealing to improve thin film uniformity and potentially cell performance. The cells were annealing for 1 hour at 125 ^{o}C in atmosphere. There was no noticeable difference in SEM images nor performance tests before and after annealing.

6.3.2 Iodine Annealing

Similarly, our group attempted iodine annealing. Substrates were attached to the bottom of a glass petri dish and flipped over so the BiI_3 film was facing downward. [28] This was placed on a hot plate with iodine crystals below and annealed at 150 ^oC for 1 hour. Again, there seemed to be no improvement in film quality or uniformity based on SEM and optical microscope analysis. These samples have not undergone performance testing yet as these steps are still in progress.

6.3.3 Solvent-Vapor Annealing

This method utilizes minor amount of solvent placed on a hot plate under a petri dish alongside the BiI_3 films. [13] In last years BiI_3 MQP this method appeared to improve the solar cell performance. The idea is that the solvent will vaporize and slightly dissolve and recrystallize the BiI_3 crystals with the aim of improving the crystal orientation and uniformity. This showed no improvement after analyzing via SEM and optical images.

6.4 Effect of CuSCN Spin-coating on BiI_3

Spin-coating CuSCN onto BiI_3 partially dissolves the BiI_3 layer and affects the film quality. Below, the left image is without CuSCN and the right image is with CuSCN. The film is thinner and less vertically oriented after CuSCN. Also, the thickness has decreased with addition of CuSCN.

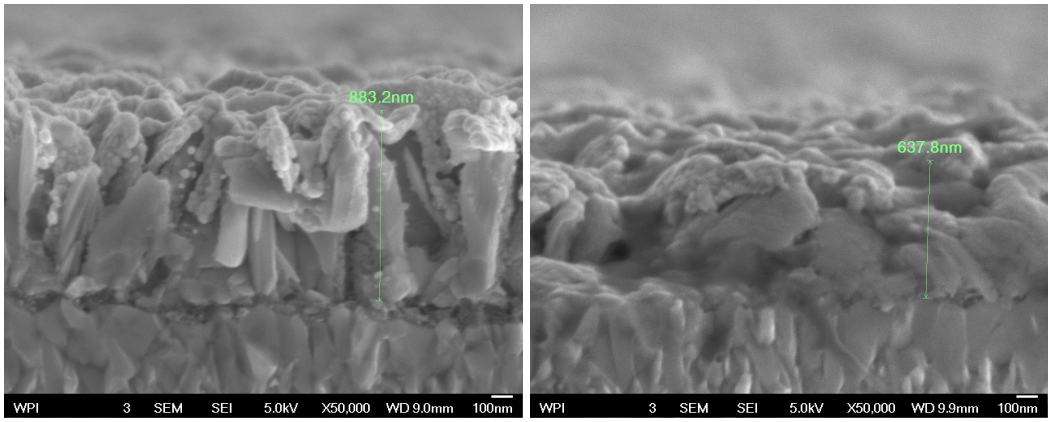

Figure 10. SEM images showing vertical BiI_3 with CuSCN deposited and with CuSCN deposited

Chapter 7: Discussion

7.1 Orientation Preference

For an absorber layer, it is vital that the film is uniform and dense. This is much more apparent in vertically oriented BiI_3 samples compared to horizontally oriented. Additionally, the horizontal samples were shiny and reflective. This makes for a poor absorber layer. There are potential avenues to overcome these downfalls of horizontal BiI_3. First, there needs to be more nucleation sites to fill in the TiO_2 substrate, and second the films need to be thinner so they are not as reflective. Some potential avenues that can be explored are higher temperatures with a shorter evaporation time. This will bombard the substrate with more vapor and potentially allow for more nucleation sites, while the decreased time will try to offset the thickness problem. Additionally, different ETL layers can be tested, although this will be challenging because TiO_2 is very well known and its procedures are consistent and pretty standard at this point.

These orientations can potentially be combined to take the best of both properties. Vertical crystals may transport charge more efficiently, and horizontal may interface better with the adjacent HTL. Combining these orientations to engineer the nanostructure at an appropriate thickness has the potential to improve BiI_3 solar cells further. Ultimately, due to the difficulties up to this point fabricating a uniform horizontal BiI_3 layer, we were not able to accurately test our hypothesis that vertical BiI_3 is the prefered orientation. However, the project will be continued through the remainder of D term with the aim of achieving an effective horizontal layer to allow for an accurate comparison of horizontal and vertical orientations.

7.2 Hole Transport Layer

One of BiI_3's biggest downfalls is its difficult in finding a compatible hole transport layer. Since it easily dissolves and evaporates, any process done for the HTL usually affects the BiI_3 layer. For example, when depositing CuI by CSS, the BiI_3 evaporated due to elevated temperatures. When spin-coating CuSCN, the BiI_3 will partially (sometimes completely) dissolve. Much more research needs to be done to find a compatible and effective hole transport layer that can be processed easily and will minimally affect BiI_3. In general, the hole transport layer is one of the major bottlenecks in BiI_3 device performance.

Chapter 8: Conclusion

In conclusion, bismuth triiodide is a uniquely processible material that can be dissolved and evaporated. In close-space sublimation, a high supersaturation will produce vertical cells and a low supersaturation will produce horizontal cells. Vertical crystals can be used to produce functioning BiI_3 solar cells that have a lot of potential for improvement. One of the major limiting factors is the HTL. Our spin-coating procedure for CuSCN likely did not uniformly coat the BiI_3 layer and potentially damaged the absorber layer. With a more uniform HTL, the performance will likely increase drastically.

While CSS can control crystal orientation based on supersaturation, the temperature difference at which the horizontal/vertical transition occurs for our process seems to occur within the 50-60 ^oC range.

In relation to our three objectives, we were able to accomplish the first one by creating a process to selectively fabricate either vertical or horizontal crystals. At this point we have only been able to partially accomplish our second objective. We haven't fully compared horizontal and vertical side by side yet, but have evidence to show that horizontal may not be able to be effectively made for solar cell usage in this process. However, there is more research that can be done to explore this further. Finally, we were able to partially accomplish the third objective thus far. While we haven't found the perfect HTL to pair with BiI_3, we have been able to deposit CuSCN in order to make functioning BiI_3 solar cells.

This is not the final submission for this project and experimentation is still continuing at this moment to to fabricate and characterize more samples to better compare horizontal and vertical orientation.

Bibliography

[1] Fossil. Department of Energy. Retrieved from: https://www.energy.gov/science-innovation/energy-sources/fossil

[2] Estimated U.S. Energy Consumption. Lawrence Livermore National Laboratories. https://flowcharts.llnl.gov/content/assets/images/charts/Energy/Energy_2017_United-States.png

[3] Kahia, M., Ben Aïssa, M. S., & Charfeddine, L. (2016). Impact of renewable and non-renewable energy consumption on economic growth: New evidence from the MENA net oil exporting countries (NOECs) doi://doi.org/10.1016/j.energy.2016.07.126

[4] Hannah Ritchie. "How long before we run out of fossil fuels?" https://ourworldindata.org/how-long-before-we-run-out-of-fossil-fuels

[5] Hannah Ritchie and Max Roser (2019) - "Energy Production & Changing Energy Sources". Published online at OurWorldInData.org. Retrieved from: 'https://ourworldindata.org/energy-production-and-changing-energy-sources' [Online Resource]

[6] Furlan, C., & Mortarino, C. (2018). Forecasting the impact of renewable energies in competition with non-renewable sources doi://doi.org/10.1016/j.rser.2017.05.284

[7] Solé, J., García-Olivares, A., Turiel, A., & Ballabrera-Poy, J. (2018). Renewable transitions and the net energy from oil liquids: A scenarios studydoi://doi.org/10.1016/j.renene.2017.09.035

[8] Climate Change Indicators: Climate Forcing. Environmental Protection Agency. https://www.epa.gov/climate-indicators/climate-change-indicators-climate-forcing

[10] Newbery, D. (2018). Evaluating the case for supporting renewable electricity doi://doi.org/10.1016/j.enpol.2018.05.029

[11] Leaman, C. (2015). The benefits of solar energy doi://doi.org/10.1016/j.ref.2015.10.002

[12] Brandt. Et al. Investigation of Bismuth Triiodide (BiI3) for Photovoltaic Applications. J. Phys. Chem. Lett. 2015, 6, 4297−4302. DOI: 10.1021/acs.jpclett.5b02022

[13] Hamdeh et al. Solution-Processed BiI3 Thin Films for Photovoltaic Applications: Improved Carrier Collection via Solvent Annealing. Chem. Mater. 2016, 28, 6567−6574. DOI: 10.1021/acs.chemmater.6b02347

[14] Boopathi et al. Solution-processable bismuth iodide nanosheets as hole transport layers for organic solar cells. Solar Energy Materials and Solar Cells, Volume 121, February 2014, Pages 35-4. DOI: https://doi.org/10.1016/j.solmat.2013.10.031

[15] The Shockley-Queisser Limit. Queen Mary University of London. https://ph.qmul.ac.uk/sites/default/files/u75/Solar%20cells_environmental%20impact.pdf

[16] Podraza et al. Band gap and structure of single crystal BiI3: Resolving discrepancies in literature. Journal of Applied Physics 114, 033110 (2013); https://doi.org/10.1063/1.4813486

[17] Huang, Zhen et al. "Highly Efficient and Stable $MAPbI_3$ Perovskite Solar Cell Induced by Regulated Nucleation and Ostwald Recrystallization" Materials (Basel, Switzerland) vol. 11,5 778. 11 May. 2018, doi:10.3390/ma11050778

[18] Saga, T. (2010). Advances in crystalline silicon solar cell technology for industrial mass production. NPG Asia Materials, 2(3), 96-102. doi:10.1038/asiamat.2010.82

[19] Green, M. A. (2009). The path to 25% silicon solar cell efficiency: History of silicon cell evolution. Progress in Photovoltaics: Research and Applications, 17(3), 183-189. doi:10.1002/pip.892

[20] Johansson et al. Extended Photo-Conversion Spectrum in Low-Toxic Bismuth Halide Perovskite Solar Cells. J. Phys. Chem. Lett. 2016, 7, 3467−3471. DOI: 10.1021/acs.jpclett.6b01452

[21] Solar energy technology basics. (2013). Retrieved from https://www.energy.gov/eere/solar/articles/solar-energy-technology-basics

[22] M. C. Wei, S. J. Chang, C. M. Lee and R. W. Chuang, "The challenge of commercialized crystalline silicon solar cell," 2008 2nd Electronics System-Integration Technology Conference, Greenwich, 2008, pp. 33-38.
DOI: 10.1109/ESTC.2008.4684319

[23] Almosni, S., Delamarre, A., Jehl, Z., Suchet, D., Cojocaru, L., Giteau, M., . . . Guillemoles, J. (2018). Material challenges for solar cells in the twenty-first century: Directions in emerging technologies. Science and Technology of Advanced Materials, 19(1), 336-369. doi:10.1080/14686996.2018.1433439

[24] Health hazards of methylammonium lead iodide based perovskites: cytotoxicity studies. http://pubs.rsc.org.ezproxy.wpi.edu/en/Content/ArticleLanding/2016/TX/C5TX00303B#!divAbstract

[25] Leguy et al. Experimental and theoretical optical properties of methylammonium lead halide perovskites. Nanoscale, 2016, 8, 6317-6327. DOI: 10.1039/C5NR05435D

[26] FIB-SEM Investigations of the Microstructure of CIGS Solar Cells. Semantic Scholar. https://pdfs.semanticscholar.org/11d3/02296964b098675511e05579a4e7df6c21f0.pdf

[26.1] W. Tress, N. Marinova, O. Inganäs, M. K. Nazeeruddin, S. M. Zakeeruddin and M. Graetzel, "The role of the hole-transport layer in perovskite solar cells - reducing recombination and increasing absorption," 2014 IEEE 40th Photovoltaic Specialist Conference (PVSC), Denver, CO, 2014, pp. 1563-1566.
doi: 10.1109/PVSC.2014.6925216

[27] Baines, T., Shalvey, T. P., & Major, J. D. (2018). In Letcher T. M., Fthenakis V. M.(Eds.), 10 - CdTe solar cells Academic Press. doi://doi.org/10.1016/B978-0-12-811479-7.00010-5

[27.1] Pitchaiya, S., Natarajan, M., Santhanam, A., Asokan, V., Yuvapragasam, A., Madurai Ramakrishnan, V., . . . Velauthapillai, D. (2018). A review on the classification of organic/inorganic/carbonaceous hole transporting materials for perovskite solar cell application doi://doi.org/10.1016/j.arabjc.2018.06.006

[28] Tiwari et al. Above 600 mV Open-Circuit Voltage BiI3 Solar Cells. ACS Energy Lett., 2018, 3 (8), pp 1882–1886 DOI: 10.1021/acsenergylett.8b01182

[28.1] Sathiyan, G., Prakash, J., Ranjan, R., Singh, A., Garg, A., & Gupta, R. K. (2018). In Bhanvase B. A., Pawade V. B., Dhoble S. J., Sonawane S. H. and Ashokkumar M.(Eds.), Chapter 9 - recent progress on hole-transporting materials for perovskite-sensitized solar cells Elsevier. doi://doi.org/10.1016/B978-0-12-813731-4.00009-6

[29] Beal et al. Cesium Lead Halide Perovskites with Improved Stability for Tandem Solar Cells. J. Phys. Chem. Lett. 2016, 7, 746−751. DOI: 10.1021/acs.jpclett.6b00002.

[29.1] Yang, X., Wang, H., Cai, B., Yu, Z., & Sun, L. (2018). Progress in hole-transporting materials for perovskite solar cellsdoi://doi.org/10.1016/j.jechem.2017.12.017

[30] J.M.K.C. Donev et al. (2018). Energy Education - Solar energy to the Earth [Online]. Available: https://energyeducation.ca/encyclopedia/Solar_energy_to_the_Earth. [Accessed: February 5, 2019].

[31] Perovskite Solar Cell. Clean Energy Institute. https://www.cei.washington.edu/education/science-of-solar/perovskite-solar-cell/

[31.1] Geography Statistics of the United States of America. World Atlas. https://www.worldatlas.com/webimage/countrys/namerica/usstates/uslandst.htm

[32] Pettersson, Andre. Bismuth(III)iodide for photovoltaic applications. (2016) https://uu.diva-portal.org/smash/get/diva2:943483/FULLTEXT01.pdf

[33] Shekar, Chandra. Unit cell and the layered structure of rhombohedral BiI3. Research Gate. https://www.researchgate.net/figure/Unit-cell-and-the-layered-structure-of-rhombohedral-BiI-3_fig1_263164724

[34] Aberle, A. G. (2009). Thin-film solar cells doi://doi.org/10.1016/j.tsf.2009.03.056

[35] Kulkarni et al. Vapor Annealing Controlled Crystal Growth and Photovoltaic Performance of Bismuth Triiodide Embedded in Mesostructured Configurations. ACS Appl. Mater. Interfaces, 2018, 10 (11), pp 9547–9554 DOI: 10.1021/acsami.8b00430

[36] Yurikawa and Murimatsu. Theoretical study of crystal and electronic structures of BiI3. J. Phys.: Condens. Matter 20 325220 http://iopscience.iop.org/article/10.1088/0953-8984/20/32/325220/pdf

[37] Tsai, Hsinhan, et al. "High-efficiency two-dimensional RuddlesdenPopper perovskite solar cells." Nature, vol. 536, no. 7616, 2016, p. 312. Expanded Academic ASAP, http://link.galegroup.com/apps/doc/A460973176/EAIM?u=mlin_c_worpoly&sid=EAIM&xid=7488b51c. Accessed 24 Feb. 2019.

[38] Cuña, A., Aguiar, I., Gancharov, A., Pérez, M., & Fornaro, L. (2004). Correlation between growth orientation and growth temperature for bismuth tri-iodide films. Crystal Research and Technology, 39(10), 899-905. doi:10.1002/crat.200410274

[39] Aggarwal, V. (2018). What are the most efficient solar panels on the market? Retrieved from https://news.energysage.com/what-are-the-most-efficient-solar-panels-on-the-market/

[39.1] Shlenskaya, N. N., Tutantsev, A. S., Belich, N. A., Goodilin, E. A., Grätzel, M., & Tarasov, A. B. (2018). Electrodeposition of porous CuSCN layers as hole-conducting material for perovskite solar cells doi://doi.org/10.1016/j.mencom.2018.07.012

[40] Huang, S., Wang, Y., Shen, S., Tang, Y., Yu, A., Kang, B., . . . Lu, G. (2019). Enhancing the performance of polymer solar cells using solution-processed copper doped nickel oxide nanoparticles as hole transport layer doi://doi.org/10.1016/j.jcis.2018.10.013

[41] Sun, M., Hu, J., Zhai, C., Zhu, M., & Pan, J. (2017). A p-n heterojunction of CuI/TiO2 with enhanced photoelectrocatalytic activity for methanol electro-oxidation doi://doi.org/10.1016/j.electacta.2017.06.035

[42] Kaushik, D. K., Selvaraj, M., Ramu, S., & Subrahmanyam, A. (2017). Thermal evaporated copper iodide (CuI) thin films: A note on the disorder evaluated through the temperature dependent electrical properties doi://doi.org/10.1016/j.solmat.2017.02.030

[43] Rajeswari, R., Mrinalini, M., Prasanthkumar, S., & Giribabu, L. (2017). Emerging of inorganic hole transporting materials for perovskite solar cells. The Chemical Record, 17(7), 681-699. doi:10.1002/tcr.201600117

[44] Ezealigo, B. N., Nwanya, A. C., Simo, A., Bucher, R., Osuji, R. U., Maaza, M., . . . Ezema, F. I. (2017). A study on solution deposited CuSCN thin films: Structural, electrochemical, optical properties doi://doi.org/10.1016/j.arabjc.2017.04.013

[45] Sepalage, G. A., Meyer, S., Pascoe, A. R., Scully, A. D., Bach, U., Cheng, Y., & Spiccia, L. (2017). A facile deposition method for CuSCN: Exploring the influence of CuSCN on J-V hysteresis in planar perovskite solar cells doi://doi.org/10.1016/j.nanoen.2016.12.043

[46] Bakr, Z. H., Wali, Q., Fakharuddin, A., Schmidt-Mende, L., Brown, T. M., & Jose, R. (2017). Advances in hole transport materials engineering for stable and efficient perovskite solar cells doi://doi.org/10.1016/j.nanoen.2017.02.025

[47] Guo, Q., Li, C., Qiao, W., Ma, S., Wang, F., Zhang, B., . . . Tan, Z. (2016). The growth of a CH 3 NH 3 PbI 3 thin film using simplified close space sublimation for efficient and large dimensional perovskite solar cells. Cambridge, UK : RSC Pub. doi:10.1039/C5EE03620H

[48] Birkett, M., Linhart, W. M., Stoner, J., Phillips, L. J., Durose, K., Alaria, J., . . . Veal, T. D. (2018). Band gap temperature-dependence of close-space sublimation grown Sb2Se3 by photo-reflectance. APL Materials, 6(8), 084901. doi:10.1063/1.5027157

[49] Solar Jobs Decline 4 Percent Nationwide, But 29 States See Jobs Growth. The Solar Foundation. https://www.thesolarfoundation.org/solar-jobs-decline-4-percent-nationwide-29-states-see-jobs-growth/

[50] The United States uses a mix of energy sources. U.S. Energy Information Administration. https://www.eia.gov/energyexplained/?page=us_energy_home

Appendix

Appendix A: Cutting and Cleaning

I. Cut FTO-Glass into 2 cm x 2.5 cm rectangles
    A. Use a ruler and marker to measure out the samples
    B. Use a blade roller to cut along the measurements
    C. Use black tool to snap the samples
        1. The crack side should be facing up

II. Cleaning
    A. Use the multimeter to find the conductive side
    B. 1:1:1 isopropyl alcohol, acetone, and DI water rinse
        1. Pour enough of mixture into a beaker for all of the samples
        2. Sonicate mixture with samples in it for 5 minutes
            a) Repeat 2 more times with fresh mixture
    C. Use acetone or ethanol with a Q-tip to clean any marker marks that are left behind
    D. Rinse with DI water
        1. Sonicate samples for 10 minutes
    E. Blow with air to dry
        1. Located in the hood

Appendix A.1: Improved Cleaning

I. Soap and water wash
    A. In a petri dish dissolve detergent in DI water
        1. Stir mixture before placing samples in
        2. Detergent will completely dissolve once sonication is done
    B. Sonicate for 30 minutes
    C. Rinse of mixture and add DI water to petri dish
        1. Never let the samples dry, keep them in DI water between cleaning steps
II. Boiling water rinse
    A. Fill a beaker with DI water
    B. Set hot plate to 200-300 ℃
    C. Place hot plate on top of hot plate
        1. DI water will boil in ~15 minutes
    D. Place samples in the beaker when water starts to boil

1. The time that the samples are left in the hot water depends on how dirty they are

E. Take samples out of beaker and place back in petri dish
    1. Use tweezers to take out samples

III. 1:1:1 isopropyl alcohol, acetone, and DI water rinse
A. Pour enough of mixture into a beaker for all of the samples
B. Sonicate mixture with samples in it for 5 minutes
    1. Repeat 2 more times with fresh mixture

IV. Use acetone or ethanol with a Q-tip to clean any marker marks that are left behind

V. Rinse with DI water
A. Sonicate samples for 10 minutes

VI. Blow with air to dry
A. Located in the hood

Appendix B: Adding the Electron Transport Layer (TiO_2)

I. Prepare solution
A. Use two vials to make separate solutions
    1. Vial 1: 0.15M
    2. Vial 2: 0.3M
B. Set pipet to 55 microliters (0.055 mL)
    1. Vial 1: one pipet of diisopropyl titanium oxide
    2. Vial 2: two pipets of diisopropyl titanium oxide
C. Add 1 mL of 1-butanol to each vial
D. Sonicate both solutions for 10 minutes

II. Spin-coating and annealing
A. Set up the spin-coating instrument
    1. RPM = 2000
    2. Time = 30 seconds
    3. Acceleration = 1000 RPM/second
B. Place a piece of tape on the edge of sample
C. Place sample in the spin-coating instrument
    1. Turn on vacuum
D. Pipet the solutions to cover the non-taped section of the samples
    1. 0.15M, then anneal for 5 minutes at 125°C
    2. 0.3M, then anneal for 5 minutes at 125°C
    3. 0.3M, then anneal for 20 minutes at 125°C
        a) After each round of annealing take off tape
        b) Let sample cool after each annealing step

c) When annealing, put sample on a piece of foil paper with a petri dish to cover it

E. Place samples in a labeled petri dish until the next layer can be added
    1. Seal-off the petri dish with parafilm tape
    2. Cover the petri dish with foil paper

Appendix C: Horizontal and Vertical Crystals - Heating Tape

Materials needed:

- 2 inch quartz tube (confirm)
- Vacuum pump
- 2 Rubber stoppers
- Heating tape
- Substrate holder (made from metal tubing)
- Substrate cover
- Powder boat
- Metal mesh (boat cover)
- Metal push-stick
- 2 Thermocouples
    - Substrate thermocouple
    - Source thermocouple
- High vacuum lubricant
- Metal wire (confirm what type)

Procedure

I. Setting up the tube
    A. Ensure that the entire quartz tube, a substrate holder, substrate cover, and rubber stoppers are cleaned.
        1. Use acetone or ethanol and cleaning tissues to clean the quartz tube.
        2. Use acetone or ethanol and kimtech wipes to clean the substrate holder, substrate cover, and rubber stoppers.
    B. Permanently insert substrate holder, metal push stick, and thermocouples through one of the rubber stoppers.
    C. Insert the vacuum line through the opposite rubber stopper.

II. Preparing the boat
    A. Add BiI_3 powder

1. Fill until about half of the boat is full.
    a) The powder is not weighed.

B. Cover the boat with wire mesh and tie down with wiring
    1. If using the boat from previous evaporation, first check that there is no bismuth metal residue
        a) If there is, prepare a new boat

III. Attaching substrate to the substrate holder
A. Place substrate on the holder
B. Pinch the substrate thermocouple between the substrate cover and substrate
    1. Make sure that the substrate cover does not cover the TiO_2 layer
C. Tie down everything with wiring

IV. Setting up the experiment
A. Insert the stopper with the vacuum line into the quartz tube
B. Place the boat towards the opposite end of the quartz tube
C. Insert the stopper with the substrate holder, metal push stick, and thermocouples into the other end
    1. Careful not to push the boat or drop the substrate
    2. Make sure that the source thermocouple is touching the bottom of the quartz tube
D. Turn on the vacuum and fully open the valve to lower the pressure in the quartz tube (250 mTorr or lower)
E. Wrap the heating tape around the quartz tube
    1. The heating tape should completely cover the area where the substrate is

V. Running the experiment (close-space sublimation)
A. Turn on the heating tape to the desired voltage
B. Do a calibration test before running a full experiment to see if (1) the thermocouples are reading accurate information and (2) what the actual temperature through the quartz tube would be
C. Wait until thermocouples reach desired temperatures and are stable
    1. Substrate: ~
    2. Source: ~
D. Push the boat using the metal push stick under the substrate and start a timer for the desired time
    1. Before moving the boat, record the substrate and source thermocouple temperatures as well as the vacuum pressure
        a) Record the temperatures and the pressure at the beginning, midway through, and at the end
E. Once the desired time has been reached, pushed the boat using the metal stick away from the heating tape and underneath the substrate

F. Turn off the heating tape
G. Open the vacuum and remove the metal push-stick from the stopper to allow the pressure inside the quartz tube to reach atmospheric pressure
H. Once atmospheric pressure is reached and the quartz tube has cooled, remove the stopped with the substrate holder and thermocouples
I. With tweezers, remove the substrate from the holder and analyze it for color, potential bismuth metal deposition, transparency, and any notable physical characteristics

Appendix D: Vertical Crystals - Hot Plate

Materials needed

- 2 inch quartz tube (confirm)
- Vacuum pump
- 2 Rubber stoppers
- Hot plate
- Substrate holder (made from metal tubing)
- Substrate cover
- Powder boat
- Metal mesh (boat cover)
- Metal push-stick
- 3 Thermocouples
    - Substrate thermocouple
    - Source thermocouple
    - Hot plate thermocouple
- High vacuum lubricant
- Metal wire (confirm what type)

Procedure

I. Setting up the tube
    A. Ensure the entire quartz tube, holder, and stoppers are cleaned
        1. Use acetone to clean everything except stoppers
        2. Stoppers are cleaned with high vacuum lubricant and wiped down with a kimtech wipe

B. Permanently insert substrate holder, metal push stick, and thermocouples through the rubber stopper
C. Insert vacuum line into the opposite rubber stopper

II. Preparing the boat
A. Add powder
1. The powder is not weighed, just added based on visually estimating half of the boat is filled with BiI_3
B. Cover boat in wire mesh and tie down with wiring
1. If using the boat from past evaporation, check that there is no Bi-metal residue

III. Attach substrate to the holder
A. Place substrate on the holder
B. Pinch thermocouple between FTO cover and substrate
C. Tie down with the wiring on the holder

IV. Setting up for the experiment
A. Make sure hotplate is under the quartz tube and stands
B. Place boat at the end of the tube
C. Carefully insert stopper with the substrate holder and push the stick into the quartz tube without touching the boat
D. Turn on the vacuum and fully open the valve to lower the pressure in the quartz tube (250 mTorr or lower)
E. Make sure that the source thermocouple is placed touching the bottom of the quartz tube where the main source of heat from the hotplate will be

V. The experiments - close space sublimation
A. Turn on the hotplate to the desired source temperature
1. Perform a calibration test before running a full experiment to see if (1) the temperature is reading accurate information and (2) what the actual temperature would be through the quartz tube
B. Lower the quartz tube to rest on the hotplate with a thermocouple resting between the hotplate and the tube
1. Center of the hotplate should be under the substrate (sample) with the boat left on the end of the tube away from the heat source
C. Wait till substrate temperature reaches equilibrium (temperature around 130 -140 °C)
D. Remove the source thermocouple out of the way
E. Push boat, using the stick, under the substrate and where the source thermocouple was
F. Start timer for the desired time

G. Record the temperature and the pressure at the beginning of the timing, midway through, and at the end
H. Once the time has been reached, pushed the boat, using the stick, away from the middle of the hotplate and from underneath the substrate
I. Move off the hotplate, turn it off, vertically
J. Open vacuum and remove the stick from the stopper allowing the pressure to get to atmospheric
K. Once cooled and at atmospheric pressure, remove the stopper with the substrate
L. Remove the sample from the holder and analyze it for color, potential Bi-metal deposition, transparency, and any notable physical characteristics

Appendix E: Gold Layer

I. Cover sample with aluminum foil
    A. Cut out two rectangular strips where the gold would be deposited
II. Let a graduate student, or known users, know that there are samples ready for gold evaporation

Appendix F: Performance Test

I. Attach sample to quartz slide using double sided tape, set up with the solar simulator for back illumination.
II. Turn on the solar simulator and load the EC Lab software. Make sure the light is not illuminating the sample yet to avoid over-exposing the sample.
III. Connect the potentiometer connections and turn on potentiometer.
IV. Connect the potentiometer to the EC Lab software
V. Run the LSV test with the appropriate voltage range
VI. Export data as a csv and convert into a graph

Appendix G: Light Absorption Test

I. Set up the integrating sphere
II. Attach sample to white cardboard to be used as sample holder.
III. Load absorbance measurement software
IV. Collect a background sample and subtract it
V. Collect the reflectance measurement spectrum
VI. Collect the transmittance spectrum
VII. Use the following equation to calculate the absorbance spectrum: $A = 1 - T - R$